Available online at www.sciencedirect.com
SCIENCE DIRECT®
Geochimica et Cosmochimica Acta 70 (2006) 1471–1482
Geochimica
www.elsevier.com/locate/gca

Zr/Rb ratio in the Chinese loess sequences and its implication for changes in the East Asian winter monsoon strength

Jun Chen [a,*], Yang Chen [a], Lianwen Liu [a], Junfeng Ji [a], William Balsam [b], Youbin Sun [a], Huayu Lu [c]

[a] *Institute of Surficial Geochemistry, State Key Laboratory of Mineral Deposit Research, Department of Earth Sciences, Nanjing University, Nanjing 210093, China*
[b] *Department of Earth and Environmental Sciences, University of Texas at Arlington, Arlington, TX 76019, USA*
[c] *State Key Laboratory of Loess and Quaternary Geology, Institute of Earth Environment, CAS, Xi'an 710075, China*

Received 2 May 2005; accepted in revised form 28 November 2005

Abstract

The long-term dust accumulation sequences on the Chinese Loess Plateau (CLP) provide a valuable opportunity to study the evolution of East Asian winter monsoon strength. Grain size of bulk samples of loess deposits, though widely used, is a modified measure of the strength of winter monsoon wind due to modification by post-depositional weathering and pedogenesis. This study proposes a new and reliable geochemical climate proxy that records the variability of the East Asian winter monsoon on the CLP. Six loess–paleosol sections on the Plateau were selected for measuring concentrations of the trace elements Zr and Rb as well as grain size. Variations of the Zr/Rb ratio in all the sections encompassing the last 130 ka display a generally similar pattern to that of mean grain size of bulk samples (MGSB). Though a positive correlation exists between the Zr/Rb ratio and MGSB, the correlation coefficient decreases in southern and eastern sections where intense pedogenesis occurred in the relatively warm and humid climates. Long-term Zr/Rb variation in the Lingtai section exhibits amplitudes and frequencies similar to those in MGSB and the mean grain size of quartz particles (MGSQ, accepted as a more reliable proxy than MGSB) in the upper loess–paleosol sequence over the past 2.6 Ma. However, for the underlying Red Clay formation, in the interval from about 7–2.6 Ma B.P., the MGSB record is relatively stable, whereas both the Zr/Rb ratio and MGSQ show distinct variability and display amplitudes similar to those observed in the overlying loess–paleosol sequence. These results demonstrate that the Zr/Rb ratio reflects original eolian grain size and may serve as a reliable index of the strength of East Asian winter monsoon winds.

1. Introduction

1.1. East Asian monsoon and loess accumulation

Meteorological studies have shown that the climate of East Asia is characterized by seasonal alternations of summer and winter monsoons, which are among the most dynamic interactions of the continent—ocean—atmosphere system in the world (Chen et al., 1991; Liu and Ding, 1998). During winter seasons, cold air from high latitudes, driven by the continental high-pressure system, extends southward along the eastern margin of the Tibetan Plateau to tropical South China and even to equatorial Indonesian Seas. These winds form the strongest northerly dry and cold winter monsoon in the world. During summer seasons, warm and humid air originating from low latitude oceans migrates northward into China's interior as far as China-Mongolia border. This warm, humid air forms the northernmost summer monsoon in the world (An, 2000).

Alternations of these monsoon systems are recognizable in geological records, especially in the well-known loess–paleosol–Red Clay sequences in central China. Numerous

* Corresponding author. Fax: +86 25 835 923 93.
E-mail address: chenjun@nju.edu.cn (J. Chen).

0016-7037/$ - see front matter © 2005 Elsevier Inc. All rights reserved.
doi:10.1016/j.gca.2005.11.029

studies of loess–paleosol sequences have shown that these deposits originate from dust accumulations transported by the northwesterly winter monsoon winds (Li et al., 1988; An et al., 1990; An, 2000). Loess was deposited at times when the winter monsoon prevailed, whereas the intercalated accretionary paleosols developed when the summer monsoon was enhanced (An et al., 1990, 1991a). Because Chinese loess–paleosol sequences continuously register the alternating rise and decline in the intensity of East Asian summer and winter monsoons, they are an excellent archive documenting the history and variability of East Asian monsoon climate extending back at least 2.5 Ma ago (An et al., 1990; Ding et al., 1994) and probably back to 22 Ma ago (Guo et al., 2002; Wang et al., 2005).

1.2. Proxies for the East Asian monsoon strength

Intensity of the East Asian paleomonsoon has been described by several proxy indices. Magnetic susceptibility signal can serve as an indicator of the summer monsoon intensity (An et al., 1991a). Grain size of bulk samples (GSB) from loess and paleosols are widely employed as proxies of the strength of winter monsoon winds. These winter monsoon proxies include median or mean grain size (An et al., 1991b; Ding et al., 1998), coarse fraction content (Porter and An, 1995; Lu et al., 1999, 2004), and grain size ratios (Ding et al., 1994; Vandenberghe et al., 1997). However, post-depositional weathering and pedogenic processes can modify the initial grain-size composition of loess deposits to various degrees (Xiao et al., 1995; Sun et al., 2000, 2006a). Therefore, GSB might represent a modified measure of the initial aeolian conditions.

In order to ascertain a more accurate history of winter monsoon variations, some researchers have tried analyzing the grain-size composition of quartz particles (GSQ) in loess and paleosols because this mineral is highly resistant to alteration in low-temperature environments (Xiao et al., 1995; An and Porter, 1997; Sun et al., 2000). Recently, Sun et al. (2006b) found that the similarity in the grain-size compositions between bulk and quartz samples decreased gradually from weakly weathered loess to weathered paleosol and then to strongly weathered Red Clay. These studies show that GSQ is more reliable than GSB in determining initial paleowind strength, especially for the Pliocene Red Clay. However, isolating quartz particles from bulk loess and paleosol samples is a complicated and time-consuming procedure, making the search for a new, more easily determined winter monsoon proxy worthwhile.

1.3. Purpose of study

Elemental analysis of sediments has been widely used to determine provenance (Fralick and Kronberg, 1997; Sun, 2002) and to evaluate paleoclimates (Gallet et al., 1996; Chen et al., 1999; Ding et al., 2001; Wehausen and Brumsack, 2002). For example, Al/K ratio changes from the suspended load of the Zaire River were interpreted as fluctuations in weathering intensity related to variations in the West African monsoon (Schneider et al., 1997); the K/Si record of ODP Site 1145 was applied to monitor terrigenous input to the northern South China Sea with a response to insolation-forced monsoon variability (Wehausen and Brumsack, 2002); and, Zr/Rb ratio in the fine-grained siliciclastics from the Barents Sea and Svalbard was interpreted as indicating grain-size variations (Dypvik and Harris, 2001). Overall, the use of element ratios can eliminate effects such as sedimentary dilution and pedogenic leaching.

In this study, we conducted analyses of Zr and Rb by X-ray fluorescence spectrometer (XRF) for the last glacial–interglacial cycle from samples in five loess–paleosol sections and in the entire 280 m Lingtai section, from the Holocene soil (S0) back to the late Tertiary Red Clay. We selected Zr and Rb to construct a new climatic proxy index because of their relatively higher concentrations and more rapid and precise measurements than other trace elements in loess, thus can obtain large-scale investigation. Here, we use these two elements to address two important questions concerning the East Asian winter monsoon: (1) during dust deposition and pedogenic processes, what is the relationship of the Zr/Rb ratio to the grain size of the initial dust and can the ratio of these two elements be considered as an indicator for wind intensity of the East Asian winter monsoon? (2) What do spatial and temporal variations of Zr/Rb ratio in loess deposits indicate about the evolution of the winter monsoon intensity?

2. Materials and methods

2.1. Materials and settings

To examine temporal and spatial variations of winter monsoon intensity, 1750 samples were collected at 12–25 cm intervals from six stratigraphic sections (Fig. 1a, Table 1). These sections are located roughly along two transects. One is north-south, including four sections near Huanxian, Xifeng, Lingtai and Baoji, respectively; the other is a west-east transect, including sections near Pingliang, Xifeng and Luochuan. All these sections are situated on the flat, broad and high tablelands. At present, both the mean annual temperature (MAT) and the mean annual precipitation (MAP) exhibit a northward and westward decrease (Porter et al., 2001). At the southernmost section, Baoji, MAT is about 13 °C and MAP is around 700 mm; whereas at the northernmost section, Huanxian, MAT and MAP decrease to about 7.6 °C and 400 mm, respectively. Relatively small decreases both in MAT and in MAP can be observed along the west-east transect (Table 1).

Pedostratigraphic units S0, L1 and S1 are well developed in the sections and can be correlated to each other in the field (Fig. 2). S0 and S1 are paleosols formed during the Holocene and last interglacial, respectively, which correspond with the marine isotope stages (MIS) 1 and 5

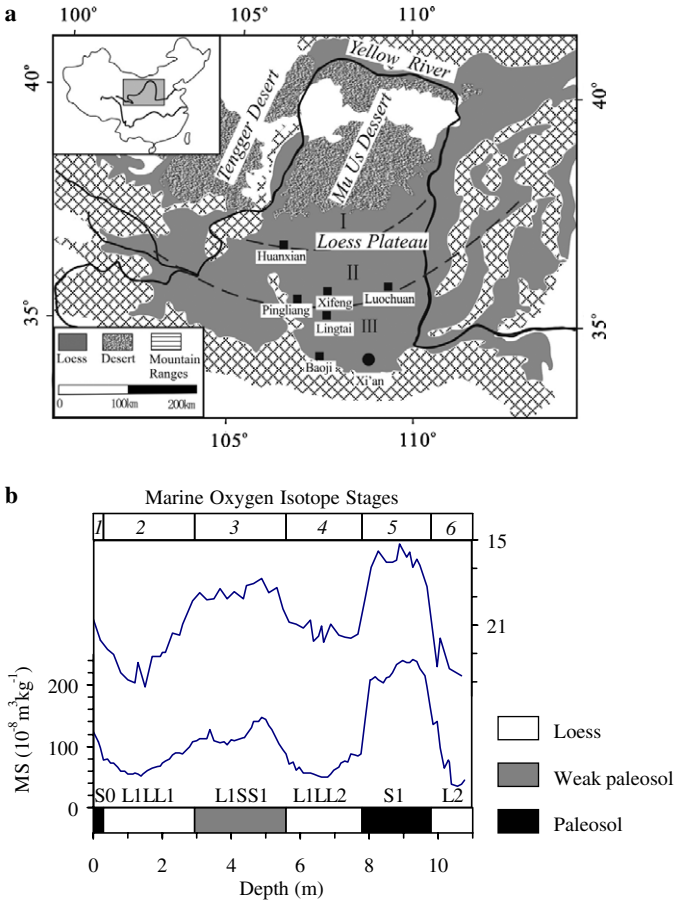

Fig. 1. Sample locations and nature of the loess deposits. (a) Index map of the Loess Plateau, showing localities of loess–paleosol sections sampled in this study. Roman numerals indicate the three zones of loess: I, sandy loess; II, silty loess and III, clayey loess (Liu, 1985). (b) Stratigraphy, variations of magnetic susceptibility (MS) and mean grain size of bulk samples (MGSB) in the typical Luochuan section shown spanning the last 130 kyr. It can be seen that the summer monsoon indicator, MS, is negatively correlated with the winter monsoon proxy, MGSB. Also, the marine isotopic stages (MIS) from 1 to 6 are shown, corresponding to stratigraphic units in the section.

Table 1
Location and climate parameters of the studied loess sections

Location	Longitude (°E)	Latitude (°N)	Thickness (m)	MAT (°C)	MAP (mm)
Huanxian	107.3	36.6	24	7.6	400
Pingliang	106.7	35.5	15	7.8	450
Xifeng	107.6	35.7	16	8.1	540
Luochuan	109.4	35.8	10	9.2	623
Baoji	107.0	34.2	10	13.0	700
Lingtai	107.5	35.0	280	10.0	650

(Fig. 1b), respectively (Liu, 1985; Ding et al., 1994). Magnetic susceptibility is higher in S0 and S1 and MGSB is smaller. L1 is a loess horizon called the Malan Loess and was deposited during the last glacial period. It consists of two primary loess units (L1LL1, L1LL2) separated by a weak soil (L1SS1) that has a slightly higher magnetic susceptibility than L1LL1 or L1LL2 and slightly finer MGSB signal. The Malan Loess is generally correlated with the MIS 2 to MIS 4 (Fig. 1b) (Liu, 1985; Ding et al., 1994).

Spatial differences in the thickness and pedogenesis of each section are apparent. For example, the Huanxian section, located near the Mu Us desert (Fig. 1a), exhibits a relatively high sedimentation rate and weak weathering; whereas, the Baoji section, located in the most southern part of the Loess Plateau, displays a lower sedimentation rate and stronger pedogenesis, relative to other sections.

To investigate long-term paleoclimatic variations, samples from the Lingtai section were collected from the modern surface to the bottom of the Red Clay formation. The Lingtai section is well-known for including the continuous loess–paleosol–Red Clay sequence and has been extensively studied in recent years (e.g., Sun et al., 1998: Ding et al., 1999, 2001; An, 2000). The upper 170 m consists of (from the surface downward) Pleistocene loess deposits containing about 40 soil horizons, including the Malan Loess (L1), Lishi Loess (S1–L15) and Wucheng Loess (S15–L33). The basal paleomagnetic age of the loess–Red Clay boundary is about 2.6 Ma. The underlying Red Clay (~120 m in thickness) is composed of more than 100 soil horizons, accumulating between ~2.6 and 7.0 Ma (Sun et al., 1998; Ding et al., 1999) (see Fig. 3).

2.2. Methods and analysis

Acid-leaching is a common method used to investigate the behavior of elements during pedological weathering (Chen et al., 1996). In this study 12 samples from the Huanxian, Xifeng and Luochuan sections were analyzed by acid leaching experiments. For each section two loess samples from L1 and two paleosol samples from S1 were selected. Each sample was first reacted with 1 mol/L acetic acid solution for 6 h under continuous agitation, and then the acid soluble residues were separated by centrifugation. The concentration of Zr and Rb was then determined in the bulk samples and in their residues.

In addition, one sample from the least weathered loess L1LL1 (with lowest magnetic susceptibility value) at Huanxian, Xifeng and Luochuan sections was selected to evaluate the effect of grain size distribution on Zr and Rb concentrations. After leaching with acetic acid to remove the carbonate, the residues were divided into five grain-size fractions (>32, 32–20, 20–8, 8–2 and <2 μm, respectively) by wet-sieving, settling and centrifuging.

Concentrations of Zr and Rb were measured using XRF. All samples were dried at 40 °C. Five grams of each sample was ground to <200 mesh (about <75 μm) in an agate mortar, and compacted into a disc. Then the concentration of Zr and Rb was determined with an ARL9800 XP + XRF at the Center of Modern Analyses, Nanjing University. The reproducibility of Zr and Rb measurements has been tested by repetitive analyses of the National Standard

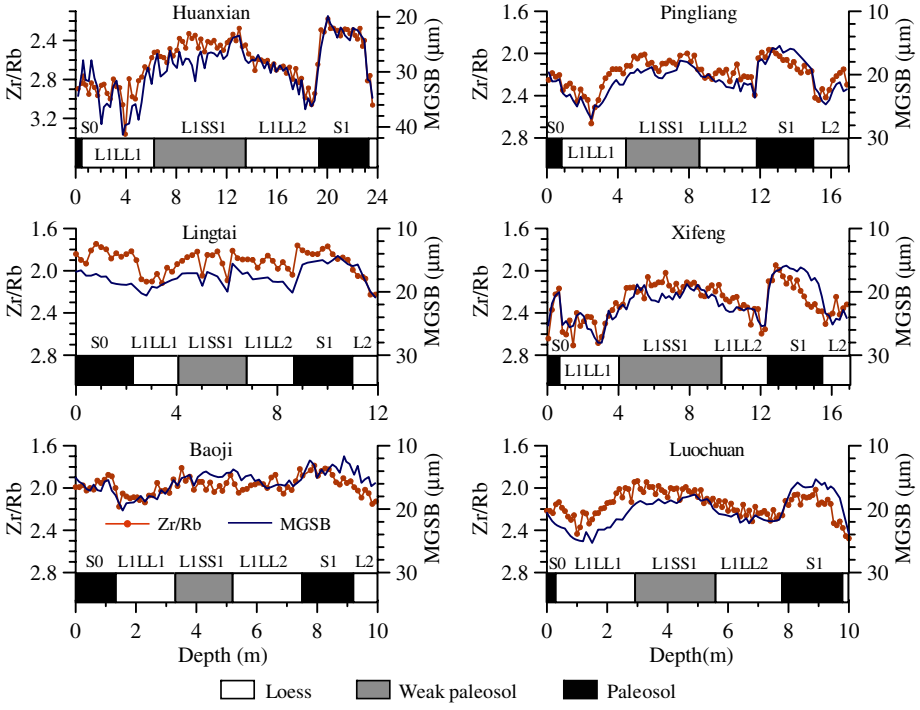

Fig. 2. Variations of the Zr/Rb ratio and MGSB in the upper part (above L2) of the six sections: HX, Huanxian; PL, Pingliang; XF, Xifeng; LC, Luochuan; LT, Lingtai; BJ, Baoji. With the exception of the Huanxian section, the Zr/Rb ratio scale is the same for all the sections.

GSS1 and GSD9; the standard deviation is about 1% and the errors estimated from the measured values and the recommended values for the standards are less than 3%.

Grain-size measurements were carried out with a Mastersizer-S laser diffraction particle analyzer at the Institute of Earth Environment, Chinese Academy of Science, Xi'an. Organic matter and carbonate were removed before examination, and then ultrasonic pretreatment in a 20% $(NaPO_3)_6$ solution was used to disperse the samples for grain-size determination. Replicate analyses show a precision of better than 4% for this procedure.

3. Results

3.1. Zr/Rb changes in loess–paleosol of the last glacial–interglacial cycle

Changes of the Zr/Rb ratio and MGSB from the six sections are illustrated in Fig. 2 and Table 2. Zr/Rb ratios display good agreement with lithostratigraphic units. For each of the studied sections, values of the Zr/Rb ratio are much higher in loess units (e.g., L1LL1, L1LL2) than in underlying soil units (e.g., L1SS1, S1). For instance, the Huanxian section, which is adjacent to the Tengger and Mu Us deserts, exhibits the weakest pedogenesis during interglacial time (Zheng et al., 1995), but there are significant differences in the Zr/Rb ratios between paleosol and loess units. The average value of the Zr/Rb ratio in L1LL1 is 2.86, whereas it is much lower in S1, only averaging 2.31. In contrast, the Baoji section, far from the deserts, exhibits a stronger intensity of pedogenesis in S1 (Rutter et al., 1991) and yields a difference of 0.2 in average Zr/Rb ratio between the paleosol (S1) and the typical loess unit (L1LL1). This difference is smaller than that (about 0.5) in the Huanxian section.

Changes of the Zr/Rb ratio exhibit a similar pattern to that of the grain size (Fig. 2), where MGSB is coarser, Zr/Rb ratio is higher. Spatial variations of the Zr/Rb ratio and grain size are clearly delineated by comparing the sections. In equivalent lithostratigraphic units, both Zr/Rb and grain size decrease along the north-south transect and are in good agreement with the distribution of three loess zones (Fig. 1a). For example, unit L1LL1 in the Huanxian section, located in the sandy loess zone, has the highest Zr/Rb value range, from 2.52 to 3.36, and the coarsest grain size, varying between 28 and 41 μm, whereas in the Lingtai section, situated in the clayey loess zone, the Zr/Rb ratio and MGSB for the same unit are much lower than in Huanxian with a range of 1.90–2.12 and 18–21 μm, respectively. These differences are most obvious in the loess units (L1LL1 and L1LL2) but are also reflected in the soil units (L1SS1 and S1).

Zr/Rb ratio and MGSB display some similarities and differences along the two transects. They are similar in the size of decrease to the south but show no obvious decrease to the east, suggesting a north-south spatial differentiation of wind sorting during aeolian transport and sedimentation. They differ in that the correspondence between the Zr/Rb and MGSB curve seems to decrease as pedogenesis increases, especially in the southern and eastern sections such as the Luochuan and Baoji.

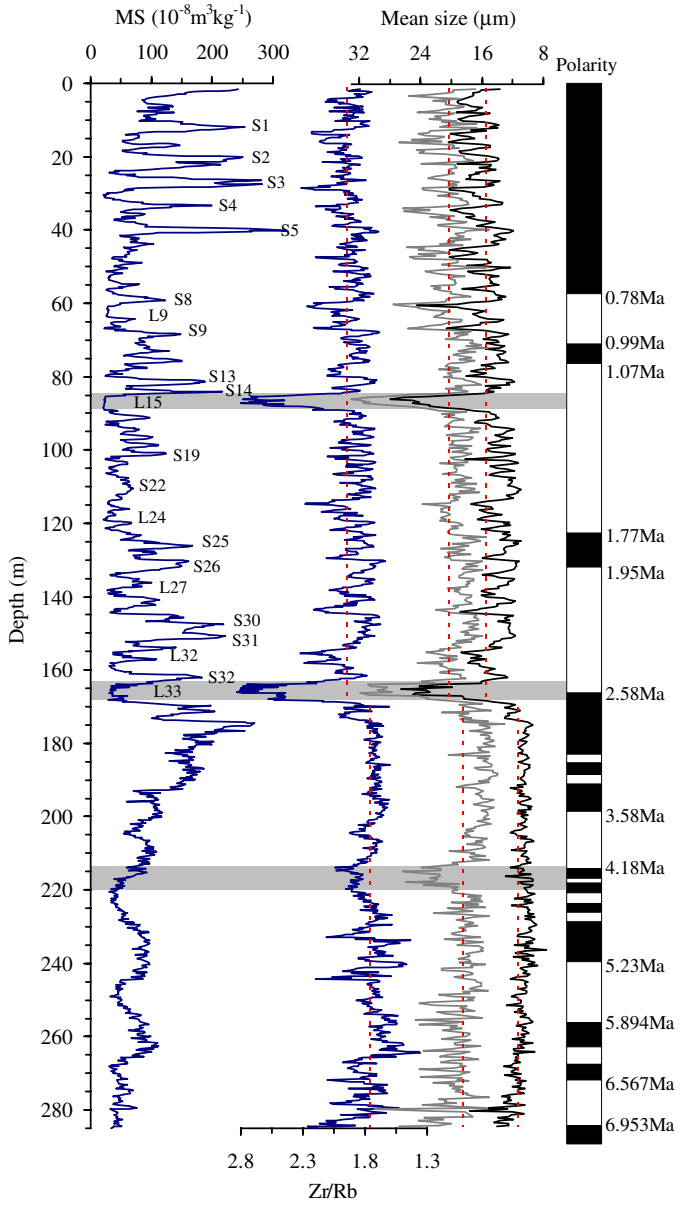

Fig. 3. Changes of Zr/Rb ratio, MGSB (dark line) and MGSQ (grey line) (Sun et al., 2006a,b) in the long-term Lingtai section, together with MS record and the magnetic polarity stratigraphy of the section (Sun et al., 1998). Dotted lines denote average values in these parameters for the loess–paleosol sequence and the Red Clay, respectively, and the shading marks the three distinctive units in the section.

3.2. Zr/Rb changes in the long-term Lingtai section

Fig. 3 shows changes in Zr/Rb ratios for the Lingtai loess-Red Clay sequence as well as MGSB and MGSQ. The Zr/Rb ratio in the 170 m of loess–paleosol sequence shows large-amplitude oscillations corresponding to loess–paleosol alternations with values being generally high in loess and lower in paleosols. In the loess–paleosol portion of the sequence, the highest Zr/Rb values occur in the two loess units, L15 and L33, with a range of 2.00–2.80, whereas in other units, the Zr/Rb record varies from 1.64 to 2.31. These increased Zr/Rb values

Table 2
Statistical results of Zr/Rb ratios and mean grain size of bulk samples (MGSB) in the last glacial–interglacial cycle of the studied loess sections

Section	Stratigraphic unit	Zr/Rb		MGSB (μm)	
		Range	Mean	Range	Mean
Huanxian	L1LL1	2.52–3.36	2.86	27.9–40.9	34.1
	L1SS1	2.28–2.63	2.45	23.4–31.7	27.4
	L1LL2	2.54–3.06	2.72	26.9–36.8	30.7
	S1	2.18–2.50	2.31	19.8–25.6	22.9
Pingliang	L1LL1	2.23–2.66	2.39	22.9–26.9	24.5
	L1SS1	2.00–2.19	2.10	17.8–22.4	19.9
	L1LL2	2.10–2.39	2.22	19.9–23.7	21.5
	S1	1.96–2.18	2.07	15.5–19.1	17.0
Xifeng	L1LL1	2.16–2.71	2.48	22.0–28.0	24.9
	L1SS1	2.01–2.26	2.15	18.8–22.8	20.4
	L1LL2	2.13–2.60	2.32	19.6–25.4	22.4
	S1	1.95–2.24	2.10	15.8–19.6	16.9
Luochuan	L1LL1	2.13–2.43	2.24	21.6–25.3	23.5
	L1SS1	1.93–2.22	2.06	17.7–21.0	19.1
	L1LL2	2.10–2.42	2.24	20.6–22.2	21.6
	S1	2.02–2.19	2.11	15.3–19.2	16.7
Lingtai	L1LL1	1.90–2.12	2.02	18.1–20.6	19.2
	L1SS1	1.81–2.09	1.89	15.6–20.0	17.5
	L1LL2	1.86–2.04	1.94	17.7–20.1	18.7
	S1	1.76–2.06	1.87	14.3–15.9	15.4
Baoji	L1LL1	1.95–2.18	2.07	15.4–20.2	18.3
	L1SS1	1.81–2.04	1.95	13.7–16.3	14.8
	L1LL2	1.88–2.05	1.98	14.6–16.7	15.8
	S1	1.79–1.97	1.87	11.7–15.8	13.5

are in agreement with the coarse grain size. MGSB and MGSQ in L15 and L33 range from 16 to 28 μm and 21 to 32 μm, respectively, whereas in other units these two measures vary from 11 to 24 μm and 15 to 28 μm, respectively. For the loess–paleosol sequence, changes in the Zr/Rb ratio are similar in amplitude and frequency to those in MGSB and MGSQ. Furthermore, the Zr/Rb ratio in loess–paleosol deposit tends to be lower with depth, coinciding with a similar trend in both MGSB and MGSQ down to the loess–Red Clay boundary.

As discussed by Sun et al. (2006a,b), MGSQ is much coarser than MGSB. Moreover, variation in MGSQ exhibits similar variability to that of MGSB and shows a good correlation with each other in the loess–paleosol sequence (Fig. 3). But, for the Red Clay formation, these two parameters display a variation that is different from the loess–paleosol sequence. Changes in the MGSB are slight, varying mostly between 8 and 13 μm. However, both MGSQ and the Zr/Rb ratio show more variability and display almost similar amplitudes to those observed in the overlying loess–paleosol sequence, mostly ranging from 14 to 25 μm and from 1.4 to 2.2 μm, respectively. Moreover, there is an increase in both the Zr/Rb and MGSQ curves at a depth of 213–221 m, which does not occur in the MGSB curve.

4. Discussion

4.1. Relationship of the Zr/Rb ratio with grain size

Geochemical composition of loess is strongly influenced by source area composition, wind transportation and post-depositional weathering and pedogenesis. Previous studies show that the source of eolian deposits has been rather constant during the Late Cenozoic time (Liu et al., 1994; Gallet et al., 1996; Ding et al., 2001). Therefore, the initial composition of loess is mainly controlled by wind sorting of dust during transportation. Stronger winter monsoon winds lead to coarser eolian dust and enrichment in coarse-grained fractions; conversely, weaker winter monsoon winds transport finer dust and lead to enrichment in fine-grained fractions.

Zr is enriched in heavy minerals in sediments, especially in zircon ($ZrSiO_4$) (Fralick and Kronberg, 1997). Rb is a typical dispersed element that is not associated with any specific Rb-bearing mineral but is present in K-containing minerals, such as K-feldspar, mica and clay minerals (Heier and Billings, 1970). The two elements are closely related to grain-size fractions in fine-grained siliciclastic sediments (Dypvik and Harris, 2001). Results from separation experiments of grain-size fractions in least weathered loess samples demonstrate that Zr and Rb are also associated with specific grain-size fractions in loess deposits (Fig. 4). Zr is enriched in the coarser fraction, whereas Rb tends to be enriched in the finer fraction. As a result, Zr/Rb ratios increase remarkably from the finest to the coarsest fraction. Moreover, Zr and Rb concentrations and Zr/Rb ratios are very similar in the same fractions within sections, indicating a good correlation between the grain-size distribution and the Zr/Rb ratio in different sections (Fig. 4).

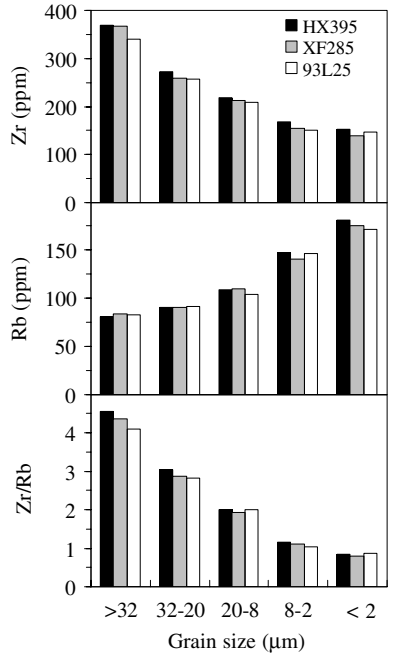

Fig. 4. Concentrations of Zr and Rb and Zr/Rb ratios in different grain-size fractions of loess samples from Huanxian, Xifeng and Luochuan sections.

Post-depositional processes such as weathering and pedogenesis may alter the initial composition of eolian deposits. As suggested by Brimhall and Dietrich (1987), the removal of soluble species in the weathering profile leads to an increase in the concentrations of relatively insoluble components. Zr is commonly used as an immobile element to evaluate the stability of other elements in soils (Bain et al., 1994; Mason and Jacobs, 1998) due to the strong resistance of zircon to chemical weathering under surface conditions (Pettijohn, 1941). Though Rb is not as stable as Zr in sediments, it is not until extensive K-feldspar alteration occurs that Rb may be removed from the weathering section and K/Rb remains unchanged during the early stages of weathering (Nesbitt et al., 1980). Mineralogical and chemical studies indicate that the intensity of weathering and pedogenesis in these eolian deposits is very weak, characterized by decalcification and calcification, while decomposition of silicate minerals is not extensive (Rutter et al., 1991; Chen et al., 1998; Han et al., 1998). Our previous data displayed slight changes of K/Rb ratio in loess and paleosol samples, all below 300, further demonstrating immobility of Rb in loess (Chen et al., 1998). Results from acid leaching experiments for both loess and paleosol samples at Huanxian, Xifeng and Luochuan sections show that removal of carbonates and other soluble phases can enrich the concentrations of Zr and Rb in loess and paleosol, but does not change the Zr/Rb ratio (Table 3). Pedogenesis may therefore alter the original concentrations of Zr and Rb in eolian dusts by relative enrichment, but during pedogenesis Zr/Rb ratios remain unchanged and reflect the initial grain size.

Linear regression analyses further confirm the positive relationship between Zr/Rb ratio and grain size (Fig. 5). However, the correlation coefficient differs among the sections suggesting a pedogenesis-induced modification of the grain-size distribution. The Huanxian section, with rather weak pedogenesis for both loess and paleosol units, exhibits the best correlation ($R^2 = 0.7764$) in the six sections; whereas the Luochuan and Baoji sections, located at the southeastern margin of the Loess Plateau where precipitation and temperature are high, yield a relative low coefficient value ($R^2 < 0.5$). Furthermore, for all the sections, the S1 of paleosol samples are located far below the trend lines in Fig. 5, indicating that pedogenesis reduces the grain size of initial eolian dusts, which is also evidenced by comparison of the grain size of bulk samples and quartz particles (see Fig. 3; Sun et al., 2006a).

The average dust accumulation rate during glacial periods on the Loess Plateau was about 0.1 mm/year, two or three times higher than during interglacial periods (Liu, 1985; Maher, 1998). After deposition, as the loess is exposed to water and atmospheric gases, minerals within the loess decompose selectively at varying rates. If the weathering zone reaches a depth of 1 m from the ground surface, as suggested by Maher (1998), the residence time

Table 3
Acid-leaching results for Zr/Rb ratios in loess and paleosol samples from the Huanxian, Xifeng and Luochuan sections

Sample	Section number	Stratigraphic unit	Bulk samples			Acid-residues			
			Zr (ppm)	Rb (ppm)	Zr/Rb	f[a] (wt.%)	Zr (ppm)	Rb (ppm)	Zr/Rb
Huanxian	HX330	L1LL1	252	88	2.86	89	280	99	2.82
	HX1645	L1LL2	249	91	2.74	87	281	104	2.70
	HX2025	S1	231	102	2.26	89	257	115	2.23
	HX2185	S1	249	105	2.38	91	270	115	2.36
Xifeng	XF225	L1LL1	230	94	2.45	87	262	108	2.43
	XF1145	L1LL2	240	96	2.50	87	272	110	2.47
	XF1285	S1	230	113	2.03	93	248	122	2.03
	XF1445	S1	245	110	2.24	94	257	116	2.22
Luochuan	93L115	L1LL1	218	97	2.25	88	250	110	2.26
	93L635	L1LL2	213	93	2.29	84	253	111	2.28
	93L735	S1	235	111	2.12	92	254	121	2.09
	93L805	S1	245	115	2.12	96	253	121	2.10

[a] f, weight percentage of the acid-residues.

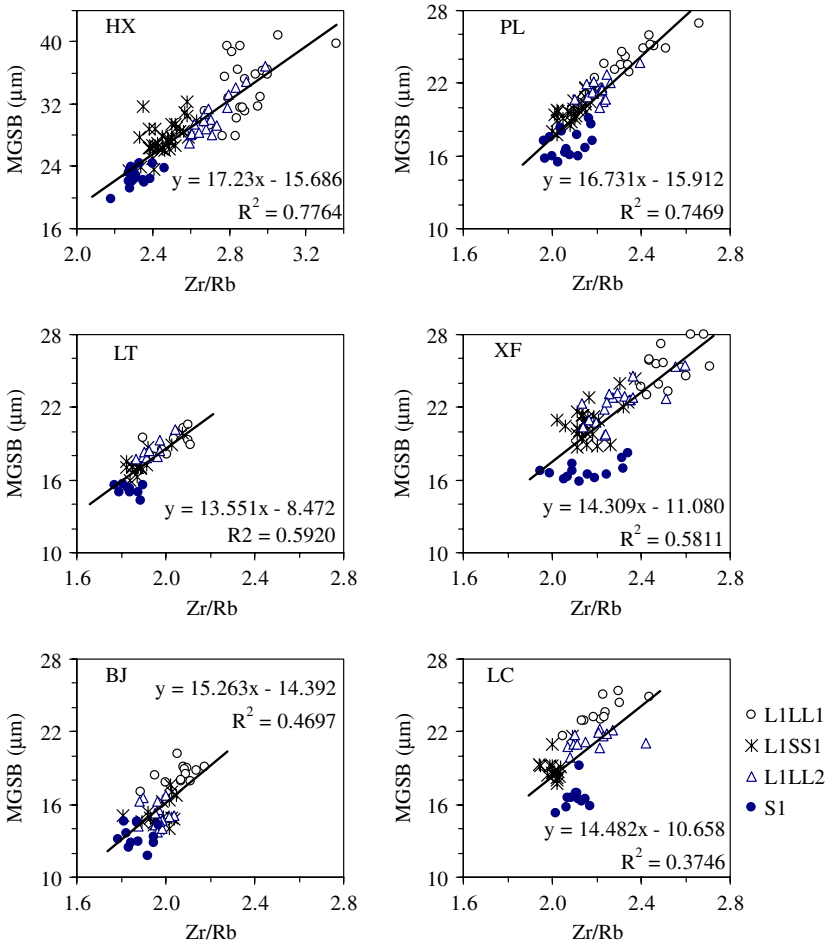

Fig. 5. Scatter plots showing the correlation between the Zr/Rb ratio and MGSB in six sections. (See Fig. 2 for locality abbreviations.)

for the loess within the zone will be about 10,000 year (at an accumulation rate of 0.1 mm/year) and even longer for the paleosols. So the pedogenic processes that produced paleosols must have been active during the accumulation of loess (Verosub et al., 1993). Loess deposition and pedogenesis were competing processes at all times, and the presence of a paleosol only indicates that the latter was predominant (An et al., 1990; Verosub et al., 1993). Hence, loess can be viewed as a kind of soil, although a very immature one (An et al., 1990).

Weathering or pedogenesis is constantly altering the initial dust grain size. That is, the measured grain size from both loess and paleosol units is not equal to the original dust grain size, but it has been altered by pedogenesis. Because the initial dust grain size is determined by the strength of the winter monsoon (Ding et al., 1994; Porter and An, 1995; Vandenberghe et al., 1997) and pedogenesis on the Loess Plateau is controlled by the oscillation of the summer monsoon (An et al., 1991a; Han et al., 1998; Ji et al., 2004), the changes in apparent grain size chronicle the alternating rise and decline in the intensity of East Asian summer and winter monsoons. Thus, the current usage of the mean grain size as a proxy for climate change will underestimate the strength of the winter monsoon during periods of paleosol development.

As mentioned above, the Zr/Rb ratios are not influenced by post-depositional processes and can be used to reflect the grain size of original eolian dust. Previous studies have demonstrated that the loess in northern China is transported mainly from deserts in the north and northwest by the winter monsoon winds (Liu, 1985; An et al., 1990). Increased winter monsoon wind strength causes coarser eolian dust to be transported and deposited. Consequently, the Zr/Rb ratio in the loess deposits can be served as a proxy of the East Asian winter monsoon wind strength.

4.2. Temporal and spatial variation of winter monsoon intensity during the last 130 ka

Provenance of Chinese loess remains controversial, although some progress on this problem has been made recently (e.g., Liu et al., 1994; Derbyshire et al., 1998; Ji et al., 1999; Sun, 2002). At present, the generally held view is that the dust is transported from the northwest to southeast (Liu, 1985) by the East Asian winter monsoon (Ding et al., 1994). However, Zr/Rb ratios in the six sections show a general southward decrease during the four marine isotopic stages (Fig. 6). For the loess units including L1LL1 and L1LL2, corresponding to MIS 2 and MIS 4, respectively, the Zr/Rb ratio decreases by about 0.33 for every one degree of decrease in latitude, whereas for the paleosol units L1SS1 and S1, corresponding to MIS 3 and MIS 5, the decrease in Zr/Rb ratios with decrease in latitude is not as large as that in loess, a gradient of about 0.2 per degree in latitude. In contrast, the spatial distribution of the Zr/Rb ratio is very similar from west to east, such as from Pinliang to Luochuan, even though the distance between them is about 300 km (see Fig. 2). This suggests that loess may have been blown from north to south and that the deserts of southern Mongolia might have been the dominant source area for the Loess Plateau, as suggested by Sun (2002). Therefore, detailed studies of the Zr/Rb parameter could provide important evidence as to the provenance of Chinese loess.

Grain size in loess sequences bears a resemblance to $\delta^{18}O$ records in deep-sea sediments (Ding et al., 1994). Using the time scale suggested by Porter and An (1995), we matched the record of Zr/Rb ratios with the SPECMAP $\delta^{18}O$ profile (Fig. 7). This comparison indicates that Zr/Rb is significantly different from the marine isotope record. For example, during MIS 3, Zr/Rb ratios of the Huanxian and Lingtai profiles (Figs. 7a and b) are quite low, even as

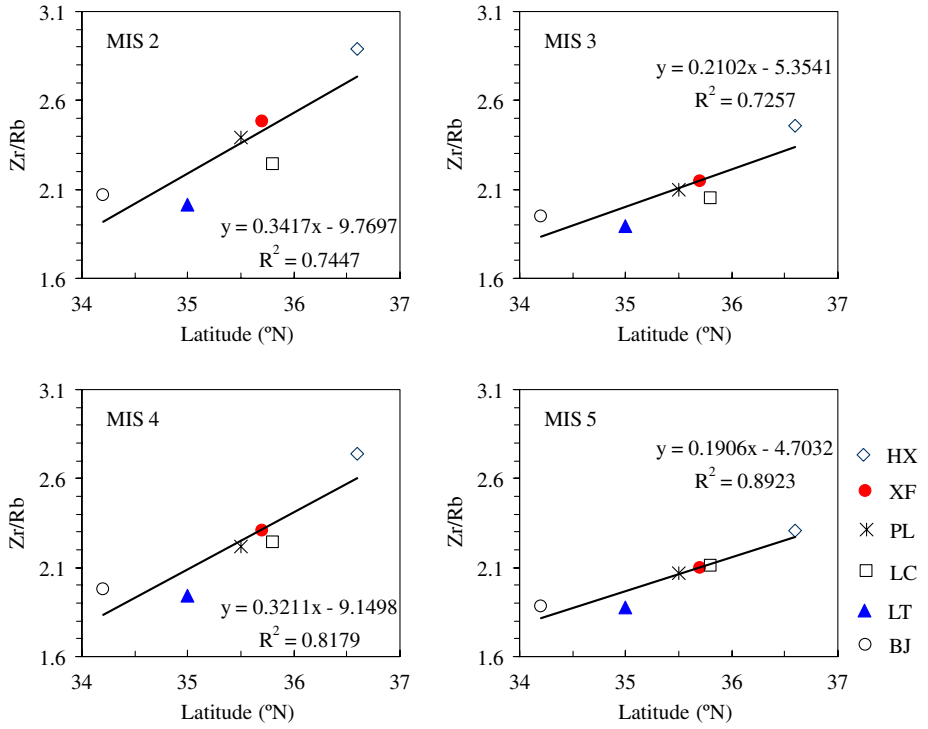

Fig. 6. Spatial variations of the average Zr/Rb ratios in six sections during MIS 2–5. (See Fig. 2 for locality abbreviations.)

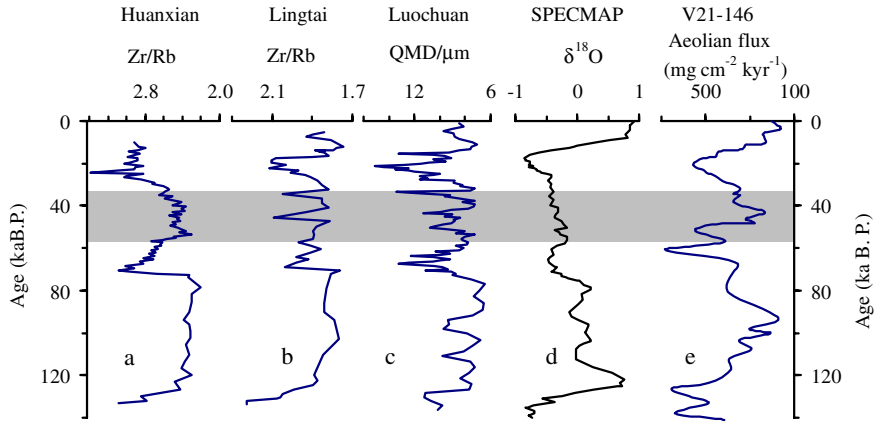

Fig. 7. Times series comparing variations of Zr/Rb ratios in the loess–paleosol sequences of Huanxian (a) and Lingtai (b) with the grain size of quartz from Luochuan (c) (Xiao et al., 1995), the SPECMAP $\delta^{18}O$ record (d) (Imbrie et al., 1984), and the dust flux record in the marine core V21–146 (e) (Hovan et al., 1991). The shading marks MIS 3.

low as the values obtained during MIS 5. This implies that the strength of the winter monsoon was relatively weak during MIS 3. The chemically isolated quartz fraction in the Luochuan section provides robust evidence for a weakened winter monsoon during MIS 3 (Fig. 7c) (Xiao et al., 1995) because the grain size of quartz particles eliminates pedogenic effects and serves as a reliable proxy for winter monsoon strength (Sun et al., 2006a,b). Evidence of Asian dust has been found down wind, far from the dust source area in western China, in Japan (Xiao et al., 1997) and in deep-sea sediments across a wide section of the North Pacific Ocean (Hovan et al., 1989, 1991; Rea, 1990). Variation of dust records in the marine core V21–146 from northwestern Pacific (Fig. 7e) (Hovan et al., 1991) shows rather low values during MIS 3, which is quite different from the marine isotope record, and exhibits a pattern that is similar to the Zr/Rb record. All of these records imply that a significant weakening of the winter monsoon intensity occurred throughout much of MIS 3.

A warm-humid climate during MIS 3 is also widely reported from other geological records, including ice cores, lake and river sediments, pollen and macrofossils, stalagmites and sea level changes. For instance, $\delta^{18}O$ values of stalagmites from Dongge Cave and Hulu Cave, China, are very similar during MIS 3 and MIS 5, indicating almost same high level of precipitation during these two intervals (Yuan et al., 2004). On the Tibetan Plateau and northwestern areas of China, these changes are attributed to higher mid- and low-latitude July-insolation than today (Shi et al., 1999, 2001). The insolation anomaly leads to enhancement of westerly circulation and summer monsoon intensity, thereby increasing the temperature and precipitation through such combined effects as reducing ice sheets and rising sea level. However, soil development is not widespread in most loess sequences on the Loess Plateau during MIS 3, and pedogenic intensity is lower than MIS 5, which contradicts the general trend of our Zr/Rb ratio data, and calls for further study in this respect.

4.3. Long-term evolution of winter monsoon strength

The Zr/Rb ratio increases gradually in the entire Lingtai section, indicating a general strengthened trend of winter monsoon intensity, which matches the global cooling indicated by oxygen isotopes from ODP cores (Shackleton et al., 1995) (Fig. 3). Comparison of the Zr/Rb ratio to MGSQ suggests the winter monsoon evolution during late Cenozoic time can be divided into four stages as marked at L15, L33 and the depth 214–220 m, respectively, which have the estimated paleomagnetic ages of about 1.2, 2.6 and 4.2 Ma B.P. at each bottom. (Fig. 3).

4.3.1. 2.6–0 Ma B.P.

The strength of winter monsoon winds exhibits waxing and waning with large amplitude and high frequency during the Quaternary, as recorded by Zr/Rb ratios, MGSB and MGSQ. Others have shown that Chinese loess sequences correlate well with marine records over the past 1.2 Ma. A cycle-to-cycle correlation can be identified between grain-size variation and the deep-sea $\delta^{18}O$ curve, suggesting dynamics of ice sheets may control the winter monsoon strength (Ding et al., 1994; Liu and Ding, 1998; Liu et al., 1999). However, in the Wucheng Formation, the lowest Quaternary loess formation, MGSB correlates ambiguously with deep-sea $\delta^{18}O$ curve. In this respect, Sun and An (2004) improved the comparison between MGSQ and deep-sea $\delta^{18}O$ records over the interval 2.6–1.6 Ma B.P. using a refined orbital timescale. Similar to MGSQ, Zr/Rb ratio also correlates well to marine oxygen isotope over the interval 2.6–1.2 Ma B.P., which extends the comparison between the continents and oceans back to 2.6 Ma B.P. (Liu et al., 2004).

Winter monsoon strength shows a strong correlation to orbital variations since 2.6 Ma B.P. As recorded by Zr/Rb ratio and MGSQ, the 400 ka eccentricity oscillation, as well as 41 ka obliquity rhythm are the dominant cycles during the interval 2.6–1.2 Ma B.P., indicating that tropical climate may play a crucial role in winter monsoon variations

through some teleconnections that amplify eccentricity forcing (Liu et al., 2004; Sun and An, 2004). Since 1.2 Ma B.P., the Zr/Rb ratio displays major 100 ka eccentricity oscillations and minor 20 ka precession frequencies suggesting that high-latitude ice volume superimposed on low-latitude ocean influence may control the East Asian winter monsoon.

4.3.2. 7.0–2.6 Ma B.P.

Previous studies have demonstrated that the Red Clay formation underlying Quaternary loess is also wind-blown in origin (Ding et al., 1998, 2001; Sun et al., 1998). But, controversy exists as to which wind system transported the Red Clay materials onto the Loess Plateau. Since MGSB in the Red Clay deposit is much finer than the Quaternary loess and displays a relatively stable pattern without distinct spatial variation, some suggest that the westerlies could have been the dominant paleowinds during the Late Tertiary in North China (Ding et al., 1998). Others argued that the Red Clay was formed mainly by low-level winter monsoon winds, based on changes in sedimentation rate and the southward decrease of MGSB and MGSQ (Sun et al., 1998; An et al., 2001; Maio et al., 2004). As illustrated in Fig. 3, unlike MGSB, the Zr/Rb ratio and MGSQ in the Red Clay at the Lingtai section show obvious variability with an amplitude similar to those observed in the overlying loess–paleosol sequence, further demonstrating that the Red Clay was also transported mainly by winter monsoon winds, which may have large amplitude and rapid frequency of variation (Sun et al., 2006b).

Using both the Zr/Rb ratio and MGSQ, the winter monsoon evolution over the 7–2.6 Ma B.P. interval can be divided into two stages. During the first stage (7–4.2 Ma B.P.), both Zr/Rb and MGSQ vary with relatively large amplitude and high frequency, suggesting larger variability of winter monsoon strength during the interval. However, the resemblance between Zr/Rb ratios and MGSQ is not as clear cut as in the overlying loess sequence, suggesting further investigation to uncover the detailed history of winter monsoon variation. During the second stage (4.2–2.6 Ma B.P.), the Zr/Rb ratio and MGSQ exhibit small variations, especially within the 3.6–2.8 Ma B.P. interval, indicating relatively weak and stable winter monsoon intensity at that time.

5. Conclusions

(1) Zr/Rb ratios in loess–paleosol sequences are sensitive to loess–paleosol alternations and are positively correlated to grain size. Because Zr and Rb are derived from an eolian source region and remain stable during the post-depositional weathering and pedogenesis, the Zr/Rb ratio is a good measure of initial dust properties which are closely related to winter monsoon strength. The Zr/Rb ratio thus provides a proxy indicator of East Asian winter monsoon circulation.

(2) Application of the Zr/Rb ratio could provide valuable information on provenance. Distribution of Zr/Rb ratios in the six sections indicates that loess materials may have been blown from north to south and that the deserts in southern Mongolia could have been the dominant source area for the Loess Plateau.

(3) Zr/Rb ratios in the loess–paleosol sequences of central China during the last 130 ka indicate that winter monsoon was relatively weak during the period of MIS 3, perhaps even as weak as during MIS 5. This implies that changes in solar insolation could play a key role in variability of the Asian monsoon at least on the orbital scale.

(4) Zr/Rb ratios, as well as MGSQ vary with large amplitude and high frequency in the Red Clay deposits, suggesting that the winter monsoon winds played a dominant role in transporting the Red Clay materials to the Loess Plateau.

Acknowledgments

This study is financially supported by the National Basic Research Program of China (Grant 2004CB720204) and the Natural Science Foundation of China (Grants 40331001 and 40173003). We are grateful to Prof. An Zhisheng for his helpful comments and to Dr. Ding Zhongli for his generous contribution of the samples from the Baoji section. We thank the Associate Editor, Dr. Martin Goldhaber, the reviewer, Prof. William C. Johnson, and other two anonymous reviewers for their thoughtful comments that significantly improved the manuscript.

Associate editor: Martin B. Goldhaber

References

An, Z.S., 2000. The history and variability of East Asian paleomonsoon climate. *Quat. Sci. Rev.* **19**, 171–187.

An, Z.S., Liu, T.S., Lu, Y.C., Porter, S.C., Kukla, G., Wu, X.H., Hua, Y., 1990. The long-term paleomonsoon variation recorded by the loess-paleosol sequence in central China. *Quat. Int.* **7**, 91–96.

An, Z.S., Kukla, G., Porter, S.C., Xiao, J.L., 1991a. Magnetic susceptibility evidence of monsoon variation on the Loess Plateau of central China during the last 130,000 years. *Quat. Res.* **36**, 29–36.

An, Z.S., Kukla, G., Porter, S.C., Xiao, J.L., 1991b. Late quaternary dust flow on the Chinese loess plateau. *Catena* **18**, 125–132.

An, Z.S., Kutzbach, J.E., Prell, W.L., Porter, S.C., 2001. Evolution of Asian monsoons and phased uplift of the Himalaya–Tibetan Plateau since late Miocene times. *Nature* **411**, 62–66.

An, Z.S., Porter, S.C., 1997. Millennial-scale climatic oscillations during the last interglaciation in central China. *Geology* **25**, 603–606.

Bain, D.C., Mellor, A., Wilson, M.J., Duthie, D.M.L., 1994. Chemical and mineralogical weathering rates and processes in an upland granitic till catchment in Scotland. *Water Air Soil Pollut.* **73**, 11–27.

Brimhall, G.H., Dietrich, W.E., 1987. Constitutive mass balance relation between chemical composition, volume, density, porosity and stain in metasomatic hydrochemical systems. *Geochim. Cosmochim. Acta* **51**, 567–587.

Chen, J., Ji, J.F., Qiu, G., Lu, H.Y., 1998. Geochemical studies on the intensities of chemical weathering in the Luochuan loess-paleosol sequence, China. *Sci. China Ser. D.* **41**, 235–241.

Chen, J., An, Z.S., Head, J., 1999. Variation of Rb/Sr ratios in the loess-paleosol sequences of central China during the last 130,000 years and their implications for monsoon paleoclimatology. *Quat. Res.* **51**, 215–219.

Chen, J., Wang, H.T., Lu, H.Y., 1996. Behaviors of REE and other trace elements during pedological weathering-Evidence from chemical leaching of loess and paleosol from the Luochuan section in central China. *Acta Geologica. Sinica.* **9**, 290–302.

Chen, L.X., Zhu, Q.G., Luo, H.B., He, J.H., Dong, M., Feng, Z.Q., 1991. *East Asian Monsoons*. Chinese Meteorological Press, Beijing (in Chinese).

Ding, Z.L., Yu, Z.W., Rutter, N.W., Liu, T.S., 1994. Towards an orbital time scale for Chinese loess deposits. *Quat. Sci. Rev.* **13**, 39–70.

Ding, Z.L., Sun, J.M., Liu, T.S., Zhu, R.X., Yang, S.L., Guo, B., 1998. Wind-blown origin of the Pliocene 'Red Clay' formation in the central Loess Plateau, China. *Earth Planet. Sci. Lett.* **161**, 135–143.

Ding, Z.L., Xiong, S.F., Sun, J.M., Yang, S.L., Gu, Z.Y., Liu, T.S., 1999. Pedostratigraphy and paleomagnetism of a ~7.0 Ma eolian loess-Red Clay sequence at Lingtai, Loess Plateau, north-central China and the implications for paleomonsoon evolution. *Palaeogeogr. Palaeoclimatol. Palaeoecol.* **152**, 49–66.

Ding, Z.L., Sun, J.M., Yang, S.L., Liu, T.S., 2001. Geochemistry of the Pliocene red clay formation in the Chinese Loess Plateau and implications for its origin, source provenance and paleoclimate change. *Geochim. Cosmochim. Acta* **65**, 901–913.

Derbyshire, E., Meng, X.M., Kemp, R.A., 1998. Provenance, transport and characteristics of modern eolian dust in western Gansu Province, China, and interpretation of the Quaternary loess record. *J. Arid Environ.* **39**, 497–516.

Dypvik, H., Harris, N.B., 2001. Geochemical facies analysis of fine-grained siliciclastics using Th/U, Zr/Rb and (Zr + Rb)/Sr ratios. *Chem. Geol.* **181**, 131–146.

Fralick, P.W., Kronberg, B.I., 1997. Geochemical discrimination of clastic sedimentary rock sources. *Sedim. Geol.* **113**, 111–124.

Gallet, S., Jahn, B., Torii, M., 1996. Geochemical characterization of the Luochuan loess-paleosol sequence, China, and paleoclimatic implications. *Chem. Geol.* **133**, 67–88.

Guo, Z.T., Ruddima, W.F., Ha, Q.Z., Wu, H.B., Qiao, Y.S., Zhu, R.X., Peng, S.Z., Wei, J.J., Yuan, B.Y., Liu, T.S., 2002. Onset of Asian desertification by 22 Myr ago inferred from loess deposits in China. *Nature* **416**, 159–162.

Han, J., Fyfe, W.S., Longstaff, F.J., 1998. Climatic implications of the S5 paleosol complex on the southernmost Chinese Loess Plateau. *Quat. Res.* **50**, 21–33.

Heier, K.S., Billings, G.K., 1970. Rubidium. In: Wedepohle, K.H. (Ed.), *Handbook of Geochemistry*, Vol. II/2. Springer-Verlag, Berlin/Heidelberg, pp. 37B1–37K3.

Hovan, S.A., Rea, D.K., Pisias, N.G., Shackleton, N.J., 1989. A direct link between the China loess and marine ^{18}O records: aeolian flux to the north Pacific. *Nature* **340**, 296–298.

Hovan, S.A., Rea, D.K., Pisias, N.J., 1991. Late Pleistocene continental climate and oceanic variability recorded in northwest Pacific sediments. *Paleoceanography* **6**, 349–370.

Ji, J.F., Chen, J., Lu, H.Y., 1999. Origin of illite in the loess from the Luochuan area, Loess Plateau, central China. *Clay Miner.* **34**, 525–532.

Ji, J.F., Chen, J., Balsam, W., Lu, H.Y., Sun, Y.B., Xu, H.F., 2004. High resolution hematite/goethite records from Chinese loess sequences for the last glacial-interglacial cycle: Rapid climatic response of the East Asian Monsoon to the tropical Pacific. *Geophys. Res. Lett.* **31**, L03207. doi:10.1029/2003GL018975.

Imbrie, J., Hays, J.D., Martinson, D.G., McIntyre, A., Mix, A.C., Morley, J.J., Pisias, N.G., Prell, W.L., Shackleton, N.J., 1984. The orbital theory of Pleistocene climate: support from a revised chronology of the marine record. In: Berge, A.L. et al. (Eds.), *Milankovitch and Climate*. Boston, Reidel, pp. 169–305, Part I.

Li, J.J., Feng, Z.D., Tang, L.Y., 1988. Late Quaternary monsoon patterns on the Loess Plateau of China. *Earth Surf. Proc. Land.* **13**, 125–135.

Liu, T.S., 1985. *Loess and the Environment*. China Ocean Press, Beijing, 251pp.

Liu, T.S., Ding, Z.L., 1998. Chinese loess and the palaeomonsoon. *Annu. Rev. Earth Planet. Sci.* **26**, 111–145.

Liu, C.Q., Masuda, A., Okada, A., Yabuki, S., Fan, Z.L., 1994. Isotopic geochemistry of Quaternary deposits from the arid lands in northern China. *Earth Planet. Sci. Lett.* **127**, 25–38.

Liu, L.W., Chen, J., Ji, J.F., Chen, Y., 2004. Comparison of paleoclimatic change from Zr/Rb ratios in Chinese loess with marine isotope records over the 2.6–1.2 Ma BP interval. *Geophys. Res. Lett.* **31**, L15204.

Liu, T.S., Ding, Z.L., Rutter, N., 1999. Comparison of Milankovitch periods between continental loess and deep sea records over the last 2.5 Ma. *Qua. Sci. Rev.* **18**, 1205–1212.

Lu, H.Y., Van Huissteden, J., An, Z.S., Nugteren, G., Vandenberghe, J., 1999. East Asia winter monsoon changes on millennial time scale before the last glacial-interglacial cycle. *J. Quat. Sci.* **14**, 101–111.

Lu, H.Y., Zhang, F.Q., Liu, X.D., Duce, R., 2004. Periodicities of palaeoclimatic variations recorded by loess-paleosol sequence in China. *Quat. Sci. Rev.* **23**, 1891–1900.

Maher, B.A., 1998. Magnetic properties of modern soils and Quaternary loessic paleosols: Paleoclimatic implications. *Palaeogeogr. Palaeoclimatol. Palaeoecol.* **137**, 25–54.

Mason, J.A., Jacobs, P.M., 1998. Chemical and particle-size evidence for addition of fine dust to soil of Midwestern United States. *Geology* **26**, 1135–1138.

Maio, X.D., Sun, Y.B., Lu, H.Y., Mason, J.A., 2004. Spatial pattern of grain size in the Late Pliocene 'Red Clay' deposits (North China) indicates transport by low-level northerly winds. *Palaeogeogr. Palaeoclimatol. Palaeoecol.* **206**, 149–155.

Nesbitt, H.W., Markovics, G., Price, R.C., 1980. Chemical processes affecting alkalis and alkaline earths during continental weathering. *Geochim. Cosmochim. Acta* **44**, 1659–1666.

Pettijohn, F.J., 1941. Persistence of heavy minerals and geologic age. *J. Geol.* **49**, 610–625.

Porter, S.C., Hallet, B., Wu, X.H., An, Z.S., 2001. Dependence of near-surface magnetic susceptibility on dust accumulation rate and precipitation on the Chinese loess plateau. *Quat. Res.* **55**, 271–283.

Porter, S.C., An, Z., 1995. Correlation between climate events in the North Atlantic and China during the last glacial. *Nature* **375**, 305–308.

Rea, D.K., 1990. Aspects of atmospheric circulation: the Late Pleistocene (0–950,000yr) record of eolian deposition in the Pacific Ocean. *Palaeogeogr. Palaeoclimatol. Palaeoecol.* **78**, 217–227.

Rutter, N., Ding, Z.L., Evans, M.E., Liu, T.S., 1991. Baoji-type pedostratigraphic section, Loess Plateau, north-central China. *Quat. Sci. Rev.* **10**, 1–22.

Schneider, R.P., Price, N.B., Müller, P.J., Kroon, D., Alexander, I., 1997. Monsoon related variations in Zaire (Congo) sediment load and influence of fluvial silicate supply on marine productivity in the east equatorial Atlantic during the last 200,000 years. *Paleoceanography* **12**, 463–481.

Shackleton, N.G., Hall, M.A., Pate, D., 1995. Pliocene stable isotope stratigraphy of ODP site 846. *Proc. Ocean Drill. Program Sci. Res.* **138**, 337–353.

Shi, Y.F., Liu, X.D., Li, B.Y., Yao, T.D., 1999. A very strong summer monsoon event during 30–40 ka BP in the Qinghai-Xizang (Tibet) Plateau and its relation to precessional cycle. *Chinese Sci. Bull.* **44**, 1851–1860.

Shi, Y.F., Yu, G., Li, X.D., Li, B.Y., Yao, T.D., 2001. Reconstruction of the 30 ~ 40 ka BP enhanced Indian monsoon climate based geological record from the Tibetan Plateau. *Palaeogeogr. Palaeoclimatol. Palaeoecol* **169**, 69–83.

Sun, D.H., Shaw, J., An, Z.S., Chen, M.Y., Yue, L.P., 1998. Magnetostratigraphy and paleoclimatic interpretation of a continuous 7.2 Ma late Cenozoic eolian sediments from the Chinese Loess Plateau. *Geophys. Res. Lett.* **25**, 85–88.

Sun, J.M., 2002. Provenance of loess material and formation of loess deposits on the Chinese Loess Plateau. *Earth Planet. Sci. Lett.* **203**, 845–859.

Sun, Y.B., An, Z.S., 2004. An improved comparison of Chinese loess with deep-sea delta O-18 record over the interval 1.6–2.6 Ma. *Geophys. Res. Lett.* **31**, L13210.

Sun, Y.B., Lu, H.Y., An, Z.S., 2000. Grain size distribution of quartz isolated from Chinese loess/paleosol. *Chinese Sci. Bull.* **45**, 2296–2298.

Sun, Y.B., Steven, C., Clemens, S.C., An, Z.S., Yu, Z.W., 2006a. Astronomical timescale and palaeoclimatic implications of stacked 3.6-Myr monsoon records from the Chinese Loess Plateau. *Quat. Sci. Rev.* **25**, 33–48.

Sun, Y.B., Lu, H.Y., An, Z.S., 2006b. Grain size of loess, palaeosol and Red Clay deposits on the Chinese Loess Plateau: significance for understanding pedogenic modification and palaeomonsoon evolution. *Palaeogeogr. Palaeoclimatol. Palaeoecol.*, accepted.

Vandenberghe, J., An, Z., Nugteren, G., Lu, H., Huissteden, K.V., 1997. New absolute time scale for the Quaternary climate in the Chinese loess region by grain-size analysis. *Geology* **25**, 35–38.

Verosub, K.L., Fine, P., Singer, M.J., Tenpas, J., 1993. Pedogenesis and paleoclimate: interpretation of the magnetic susceptibility record of Chinese loess-paleosol sequences. *Geology* **21**, 1011–1014.

Wang, P.X., Clemens, S., Beaufort, L., Braconnot, P., Ganssen, G., Jian, Z.M., Kershaw, P., Sarnthein, M., 2005. Evolution and variability of the Asian monsoon system: state of the art and outstanding issues. *Quat. Sci. Rev.* **24**, 595–629.

Wehausen, R., Brumsack, H.-J., 2002. Astronomical forcing of the East Asian monsoon mirrored by the composition of Pliocene South China Sea sediments. *Earth Planet. Sci. Lett.* **201**, 621–636.

Xiao, J.L., Porter, S.C., An, Z.S., Kumai, H., Yoshikawa, S., 1995. Grain size of quarts as an indicator of winter monsoon strength on the Loess Plateau of central China during the last 130,000 yr. *Quat. Res.* **43**, 22–29.

Xiao, J.L., Kumai, H., Yoshikawa, S., Masuda, H., An, Z.S., 1997. Eolian quartz flux to lake Biwa, central Japan, over the past 145,000 years. *Quat. Res.* **48**, 48–57.

Yuan, D., Cheng, H., Edwards, R.L., Dykoski, C.A., Kelly, M.J., Zhang, M., Qing, J., Lin, Y., Wang, Y., Wu, J., Dorale, J.A., An, Z., Cai, Y., 2004. Timing, duration, and transitions of the last interglacial Asian monsoon. *Science* **304**, 575–578.

Zheng, H., Rolph, T., Shaw, J., An, Z.S., 1995. A detailed paleomagnetic record for the last interglacial period. *Earth Planet. Sci. Lett.* **133**, 339–351.